A Wideband Decoupling Technique for Two Inverted-F Antennas Using a Capacitively Loaded Ground Cut

Wei Tang, *Student Member, IEEE*, Jiangwei Sui, *Member, IEEE*, Junru Li, *Member, IEEE*, Du Li, *Member, IEEE*, and Xiangwei Zhu, *Member, IEEE*

***Abstract*—In this letter, an efficient wideband decoupling technique is introduced for two inverted-F antennas (IFAs). By introducing a capacitively loaded ground cut, two extra coupling paths can be exploited and co-tuned to mitigate the mutual coupling between two IFAs at two frequencies. Therefore, two transmission zeros can be obtained so that a wideband and deep decoupling is achieved. An equivalent circuit is presented for the proposed antennas to reveal the decoupling mechanism. Three examples are designed to justify the proposed method, showing that wideband isolation and impedance matching are obtained with 19.6 % fractional bandwidth for 30 dB isolation and 11.2 % for 40 dB isolation. Moreover, the average total efficiency is 86% with the size of the decoupling structure only about 0.04 × 0.06 λ^2.**

***Index Terms*—Antenna decoupling, equivalent circuits, in-band full-duplex (IBFD), inverted-F antenna (IFA), multiple-input multiple-output (MIMO), mutual coupling, wideband.**

I. Introduction

TO SATISFY the requirements of large channel capacity, wideband antennas are largely used in modern wireless communication systems. To further improve the system's data throughput, the multiple-antenna scheme is another enabling technique. On one hand, the multiple-input multiple-output (MIMO) scheme has become a key technology in mobile terminals by exploiting spatial multiplexing [1]. On the other hand, the in-band full-duplex (IBFD) or simultaneous transmit and receive (STAR) scheme has drawn great attention as a promising method to double the spectral efficiency [2]. However, for both the MIMO and IBFD systems, the antennas work in the same band, which involves undesired interference between the antennas since multiple antennas need to coexist in the limited terminal space. For MIMO systems, it has been studied that 20 dB isolation is required for MIMO antennas to achieve satisfactory system performance [3]. For IBFD systems, a high isolation of 40 dB is usually required for the transmit and receive antennas to reduce the burden of the latter analog and digital domain interference mitigation.

To eliminate the mutual coupling, various decoupling techniques have been proposed, such as using neutralization structures [4], [5], special ground structures [6] – [9], parasitic decoupling elements [10], [11], decoupling networks [12] – [15], orthogonal modes [16], [17], and so on. In [18], a capacitor together with the connected branch is used to form a band-pass resonant structure to attract the coupling current to the ground. Although these methods can effectively reduce the mutual coupling and some can support the wideband scenarios [4], [5], [8], [15], [16], they mainly focus on the MIMO application about 20 dB isolation, and it is challengeable to be applied to the wideband IBFD scenarios whose requirement for antenna ports is higher than 40 dB. Among various multiple antennas in mobile terminals, the inverted-F antenna (IFA) is one of the most competitive choices due to its low profile, compactness, and simple structure [19]. Correspondingly, many great decoupling efforts have been devoted to IFA systems [20] – [29]. Specifically, a new decoupling concept named self-curing has been proposed in [27] and [28] by using capacitive elements to mitigate the coupling between IFAs. In [29], the inherent high-order ground currents are ingeniously used to reduce the mutual coupling of two IFAs. However, the ground currents are fixed if the ground plane is set, which lacks tuning flexibility. Moreover, these previous techniques just apply to a narrow band that cannot support wideband wireless communications.

In this letter, a new decoupling method is proposed to reduce the mutual coupling between two IFAs for both MIMO and IBFD scenarios. A capacitively loaded ground cut is introduced to generate two non-resonant extra coupling paths to mitigate the mutual coupling at two frequencies within the band. Compared with the existing decoupling techniques, there are mainly three contributions of the proposed method:

1) two extra non-resonant coupling paths are introduced to generate two transmission zeros for wideband decoupling and the equivalent circuit is studied in detail;

2) it can achieve wideband decoupling with isolation higher than 40 dB for IBFD applications; and

3) the introduced ground cut is quite compact for miniaturization requirements.

Manuscript received xxxx xx, 2024; accepted xxxx. This work was supported in part by the National Key R&D Program of China under Grant 2021YFA0716500, in part by the National Natural Science Foundation of China under Grant 62201625, and in part by Guangdong Basic and Applied Basic Research Foundation under Grant 2021A1515110728. (*Corresponding author: Jiangwei Sui*.)

The authors are with the School of Electronics and Communication Engineering, Shenzhen Campus of Sun Yat-sen University, Shenzhen 518000, China (e-mail: tangw29@mail2.sysu.edu.cn; suijw@mail.sysu.edu.cn; lijr85 @mail.sysu.edu.cn; lidu5@mail.sysu. edu.cn; zhuxw666@mail.sysu.edu.cn).

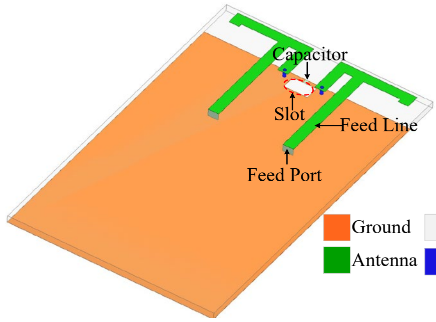

(a)

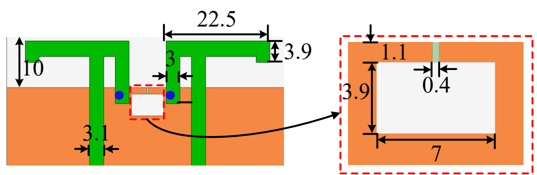

(b)

Fig. 1. Schematic geometry of the proposed planar wideband IFAs. (a) Perspective view. (b) Detailed dimensions. The unit used here is mm. The eventual capacitor value is 0.2 pF.

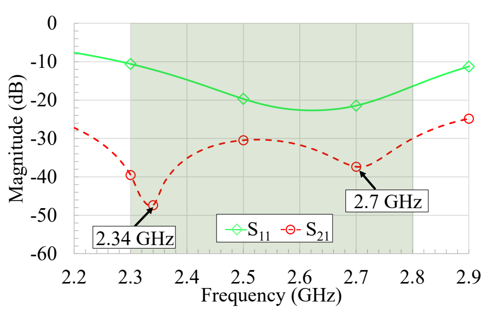

Fig. 2. Simulated S-parameters of the proposed planar wideband IFAs.

II. Antenna Geometry and Working Mechanism

As the schematic geometry shown in Fig. 1, two IFAs are located on the top side of the PCB board symmetrically. The PCB board is an FR4 substrate with a permittivity of 4.2 and a loss tangent of 0.02. A small rectangle is cut from the ground and a capacitor is inserted between the two branches stretched from the ground cut, forming a capacitively loaded ground cut. Fig 2 shows the simulated S-parameters of the proposed IFAs when a 0.2-pF capacitor is loaded on the ground cut, where there are two transmission zeros at 2.34 GHz and 2.7 GHz.

To reveal the decoupling mechanism, an equivalent circuit of the proposed planar wideband IFAs is depicted in Fig. 3, in which M_0 represents the original coupling of the coupled IFAs without the proposed capacitively loaded ground cut. By fitting the EM-simulated S-parameters and the equivalent circuit models of the antennas, the component values of the equivalent circuit can be obtained, as listed in Table I. As compared in Figs. 4(a) and 4(b), for the coupled IFAs, the S-parameters of the equivalent circuit and the EM simulated antennas agree very well for both the magnitude and phase. For the decoupled case in Figs. 4(c) and 4(d), which introduce the proposed decoupling structure, the results also coincide well with each other.

To achieve two transmission zeros, the original coupling M_0 and the two introduced coupling on the two paths, M_1 and M_2, need to be canceled with each other as follows

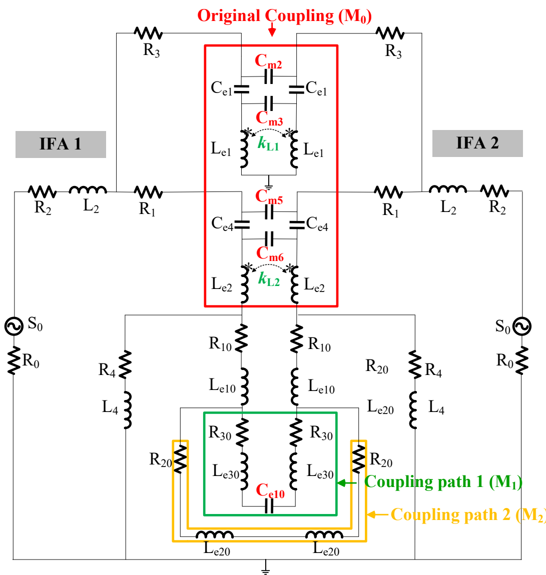

Fig. 3. An equivalent circuit of proposed planar wideband IFAs.

TABLE I
ELEMENT VALUES OF THE EQUIVALENT CIRCUIT IN THE WIDE BAND
(UNITS FOR R, L, AND C ARE Ω, NH, AND PF.)

Decoupled Antennas											
Coupled Antennas								Decoupling Part			
R_1	64	R_2	17.1	R_3	0.91	R_4	0.01	R_{10}	6	R_{20}	12.4
L_{e1}	3	L_2	3.8	L_{e2}	2.3	`L_4	2.4	R_{30}	20	L_{e10}	0.14
C_{e1}	0.59	C_{m2}	0.41	C_{m3}	0.78	k_{L1}	0	L_{e20}	2.15	L_{e30}	2.1
C_{e4}	8.42	C_{m5}	0.004	C_{m6}	0.71	k_{L2}	0	C_{e10}	0.2		

$$M_0(f_1)+M_1(f_1)+M_2(f_1)=0 \quad (1a)$$

$$M_0(f_2)+M_1(f_2)+M_2(f_2)=0 \quad (1b)$$

where f_1 and f_2 represent the two frequencies for the two transmission zeros. For the two introduced coupling, M_1 represents the capacitor path and M_2 represents the ground cut path. It can be found from Formula (1) that the total mutual coupling can be mitigated at two different frequencies by finely tuning the parameters of the capacitively loaded ground cut to adjust the corresponding M_1 and M_2 so that two zeros can coexist within a bandwidth to achieve wideband decoupling. The input susceptances of the two introduced coupling paths are calculated and depicted in Fig. 5 according to the equivalent circuit. It is found that the introduced extra coupling paths are both not resonant, with the first coupling path capacitive and the second coupling path inductive.

In another aspect, the total mutual couplings at the two frequencies can be re-formulated as follows

$$M_{total}(f_1)=M_0(f_1)+M_1(f_1)+M_2(f_1) \quad (2a)$$

$$M_{total}(f_2)=M_0(f_2)+M_1(f_2)+M_2(f_2). \quad (2b)$$

It is found that for f_1, both the M_1 (capacitance) and M_2 (ground cut) coupling paths can affect the eventual total coupling, which also applies to the case of f_2, so the two transmission zeros will be co-controlled by the capacitor value and the cut depth. To justify this hypothesis, the capacitor value and the

This article has been accepted for publication in IEEE Antennas and Wireless Propagation Letters. This is the author's version which has not been fully edited and content may change prior to final publication. Citation information: DOI 10.1109/LAWP.2024.3423364

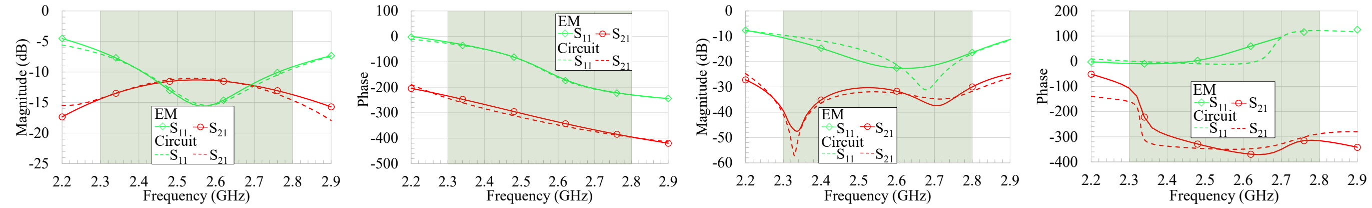

(a) (b) (c) (d)

Fig. 4. Magnitude and phase of the equivalent circuit and EM simulated S-parameters of the proposed planar wideband IFAs. (a) The magnitude of the coupled IFAs. (b) The phase of the coupled IFAs. (c) The magnitude of the decoupled IFAs. (d) The phase of the decoupled IFAs.

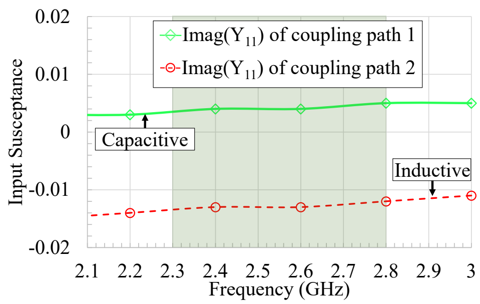

Fig. 5. Simulated input susceptances of the two introduced coupling paths.

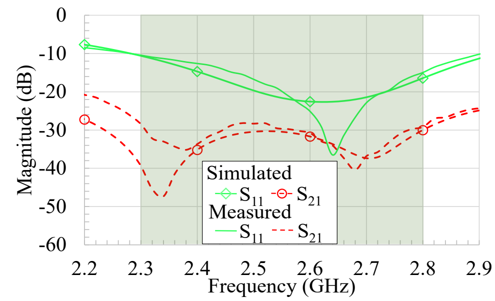

Fig. 7. Simulated and measured S-parameters of the proposed planar wideband IFAs.

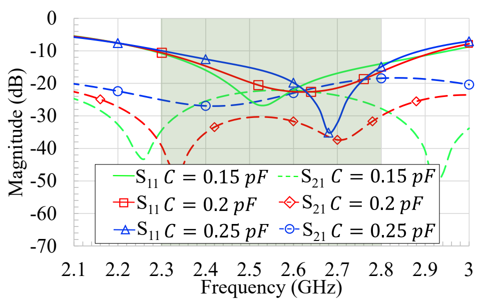

Fig. 6. Simulated S-parameters with different capacitor values.

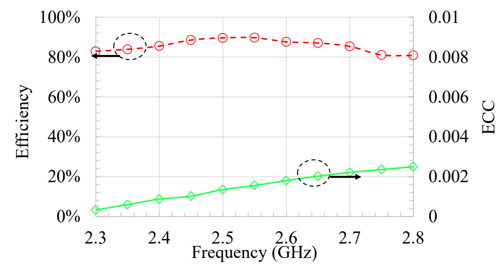

Fig. 8. Measured total efficiencies and calculated ECCs of the proposed wideband planar IFAs.

depth of the ground cut are parametrically investigated. As shown in Fig. 6, when the capacitor value is tuned, the two transmission zeros both vary, demonstrating that the first coupling path affects the total couplings at the two frequencies simultaneously, as has been revealed from Formula (2). A similar conclusion is obtained for the depth of the ground cut, and the result is omitted here for brevity. Therefore, to achieve the transmission zeros at the pre-defined f_1 and f_2, the capacitance and the ground cut require to be co-tuned.

III. Results and Discussions

A. Planar Wideband IFAs

The above-studied planar wideband IFAs are fabricated and measured. As is shown in Fig. 7, the measured results agree well with the simulated ones. It can be seen that the impedance matching is better than -10 dB from 2.3 to 2.8 GHz with the mutual coupling lower than -28 dB, which is quite good for MIMO applications. It should be noted that both the lumped and distributed capacitors can achieve the eventual decoupling, and the capacitor kind and configuration can be selected according to the specific scenarios.

It is well known that total efficiency is a vital figure of merit for terminal antennas. As shown in Fig. 8, an average value of about 86% is eventually achieved. The envelope correlation coefficient (ECC) is calculated using the measured far-field electric fields and also depicted in Fig. 8. It is found that the ECC is lower than 0.003, showing a very low spatial correlation for MIMO applications.

B. IBFD Wideband IFAs

Although 28 dB isolation has been achieved for two IFAs in the above example, it is still not enough to satisfy the 40 dB isolation requirement in the IBFD systems. To justify the generality, the two IFAs studied in the above Part A are re-studied in this part, with only the capacitively loaded ground cut fine-tuned to enhance the isolation. The eventual dimensions are marked in Fig. 9. As can be seen from Fig. 10, isolation between two IFAs is better than 40 dB from 2.36 to 2.64 GHz with the impedance matching better than -10 dB. The fractional bandwidth of about 11.2 % is achieved by using the proposed decoupling method, which will greatly reduce the complexity and cost of the whole IBFD system. Moreover, two transmission zeros are still retained within the band.

C. Vertical Wideband IFAs

To cope with the demand for wideband antennas in vertical application scenarios, the planar wideband antenna is constructed into a vertical-placed model. As is shown in Fig. 11, an FR4 substrate with a dimension of 135 × 75 × 1.6 mm^3 is designed as the mainboard with a metal ground etched on its bottom and a vertically placed sideboard of 7 mm in height.

This article has been accepted for publication in IEEE Antennas and Wireless Propagation Letters. This is the author's version which has not been fully edited and content may change prior to final publication. Citation information: DOI 10.1109/LAWP.2024.3423364

TABLE II
COMPARISON WITH SOME STATE-OF-THE-ART WIDEBAND DECOUPLING TECHNIQUES

Ref.	Decoupling Method	Transmission Zero Number	30 dB Isolation Bandwidth (%) (1)	40 dB Isolation Bandwidth (%) (1)	Measured Total Efficiency	Structure Size (λ)(2)
[5]2017	Neutralization Structure	2	19	1.5	67% – 84%	0.06
[15]2020	Decoupling networks	2	5.7	--	75% – 85%	0.1
[26]2021	Shorting stub	2	--	--	40% – 78%	0.07
[28]2022	Decoupling capacitors	1	--	--	42% –76 %	0.14
[29]2018	Ground high-order mode	1	4.3	--	--	--
Proposed	Coupling path cancellation	2	19.6	11.2(3)	81% – 91%	0.06

(1) The isolation bandwidth is under the condition that the matching condition is better than -10 dB. (2) This size denotes the longest edge of the structure. (3) This value is for the second IBFD example, whose capacitive capacitively loaded ground cut is slightly tuned from the first demonstrational example.

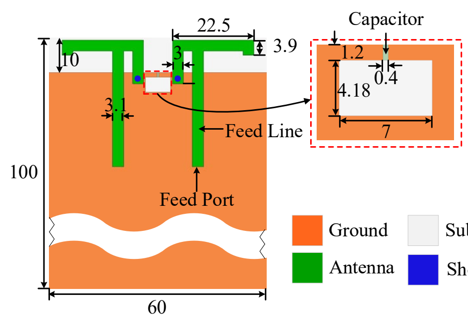

Fig. 9. Geometry of the proposed IBFD wideband IFAs. The unit used here is mm. The value of the capacitor is 0.21 pF.

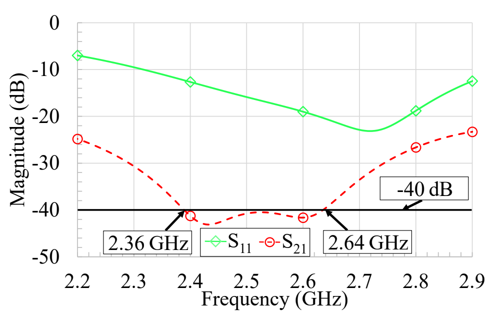

Fig. 10. Simulated S-parameters of the proposed IBFD wideband IFAs.

It is seen from Fig. 12 that the matching condition is better than -10 dB in the wide N78 band from 3.3 to 3.8 GHz and the isolation is better than 20 dB with two transmission zeros.

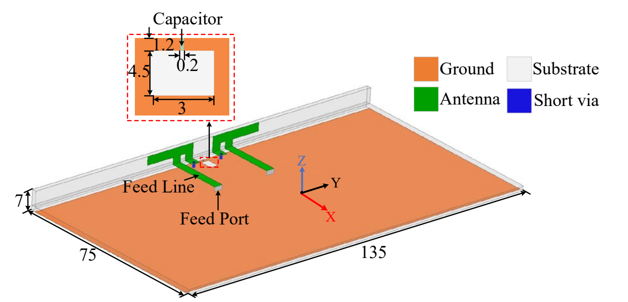

Fig. 11. Geometry of the proposed vertical-placed wideband IFAs. The unit used here is mm. The value of the capacitor is 0.1 pF.

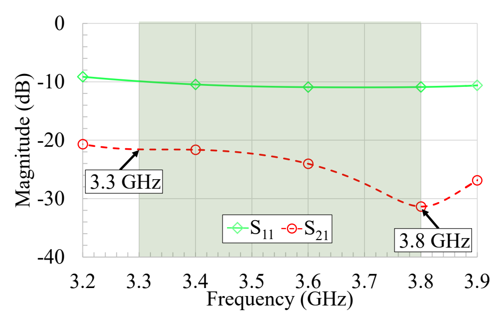

Fig. 12. Simulated S-parameters of the proposed vertical-placed wideband IFAs.

D. Comparison

The main features of the prior methods and this work are compared in Table II. Although two transmission zeros are also generated in [5], [15], and [26], their isolation bandwidth is narrower than the proposed scheme. Particularly, for IBFD applications, only the design in [5] can satisfy the 40-dB isolation requirement with a fractional bandwidth of about 1.5 %, which is too narrow to support wideband IBFD applications. In the proposed method, two transmission zeros are generated to achieve the wideband high isolations, 19.6 % for 30 dB isolation and 11.2 % for 40 dB isolation. Although the capacitor structures are also utilized in [18], [27], and [28], they are all resonant to trap the coupling current from flowing to another port, which is different from the coupling cancellation principle of the proposed non-resonant structures. Moreover, the occupied size is smaller than the prior works with a higher total efficiency.

IV. CONCLUSION

In this letter, a novel wideband decoupling scheme is proposed for two IFAs by introducing a capacitively loaded ground cut that generates two non-resonant coupling paths. By properly tuning the parameter values of the structure, the introduced two couplings can be canceled with the origin coupling at two frequencies simultaneously to achieve wideband and deep decoupling. The results show that the planar wideband example can achieve 30 dB isolation and -10 dB impedance matching within a 19.6 % fractional bandwidth. In addition, 40 dB isolation is realized of about 11.2 % fractional bandwidth for IBFD systems.

References

[1] X. Chen, S. Zhang, and Q. Li, "A review of mutual coupling in MIMO systems," *IEEE Access*, vol. 6, pp. 24706–24719, 2018.

[2] K. E. Kolodziej, B. T. Perry, and J. S. Herd, "In-band full-duplex technology: techniques and systems survey," *IEEE Trans. Microw. Theory Techn.*, vol. 67, no. 7, pp. 3025–3041, Jul. 2019.

[3] X. Mei and K.-L. Wu, "How low does mutual coupling need to be for MIMO antennas," *Proc. IEEE Int. Symp. Antennas Propag. USNC/URSI Nat. Radio Sci. Meeting,* Boston, MA, USA, pp. 1579–1580, 2018.

[4] Y. Wang and Z. Du, "A wideband printed dual-antenna with three neutralization lines for mobile terminals," *IEEE Trans. Antennas Propag.*, vol. 62, no. 3, pp. 1495–1500, Mar. 2014.

[5] C.-D. Xue, X. Y. Zhang, Y. F. Cao, Z. Hou, and C. F. Ding, "MIMO antenna using hybrid electric and magnetic coupling for isolation enhancement," *IEEE Trans. Antennas Propag.*, vol. 65, no. 10, pp. 5162–5170, Oct. 2017.

[6] L. Zhao, Y. He, G. Zhao, X. Chen, G. -L. Huang, and W. Lin, "Scanning angle extension of a millimeter-wave antenna array using electromagnetic band gap ground," *IEEE Trans. Antennas Propag.*, vol. 70, no. 8, pp. 7264-7269, Aug. 2022.

[7] M. S. Sharawi, A. B. Numan, M. U. Khan, and D. N. Aloi, "A dual-element dual-band MIMO antenna system with enhanced isolation for mobile terminals," *IEEE Antennas Wireless Propag. Lett.*, vol. 11, pp. 1006-1009, 2012.

[8] J.-F. Li, Q.-X. Chu, and T.-G. Huang, "A compact wideband MIMO antenna with two novel bent slits," *IEEE Trans. Antennas Propag.*, vol. 60, no. 2, pp. 482–489, Feb. 2012.

[9] Y. Q. Hei, J. G. He, and W. T. Li, "Wideband decoupled 8-element MIMO antenna for 5G mobile terminal applications," *IEEE Antennas Wireless Propag. Lett.*, vol. 20, no. 8, pp. 1448-1452, Aug. 2021.

[10] A. C. K. Mak, C. R. Rowell, and R. D. Murch, "Isolation enhancement between two closely packed antennas," *IEEE Trans. Antennas Propag.*, vol. 56, no. 11, pp. 3411–3419, Nov. 2008.

[11] B. K. Lau and J. B. Andersen, "Simple and efficient decoupling of compact arrays with parasitic scatterers," *IEEE Trans. Antennas Propag.*, vol. 60, no. 2, pp. 464-472, Feb. 2012.

[12] S. C. Chen, Y. S. Wang, and S. J. Chung, "A decoupling technique for increasing the port isolation between two strongly coupled antennas," *IEEE Trans. Antennas Propag.*, vol. 56, no. 12, pp. 3650–3658, Dec. 2008.

[13] J. Sui and K.-L. Wu, "A general T-stub circuit for decoupling of two dual-band antennas," *IEEE Trans. Microw. Theory Techn.*, vol. 65, no. 6, pp. 2111–2121, Jun. 2017.

[14] M. Li, L. Jiang, and K. L. Yeung, "Novel and efficient parasitic decoupling network for closely coupled antennas," *IEEE Trans. Antennas Propag.*, vol. 67, no. 6, pp. 3574-3585, June 2019.

[15] Y.-F. Cheng and K.-K. M. Cheng, "Compact wideband decoupling and matching network design for dual-antenna array," *IEEE Antennas Wireless Propag. Lett.*, vol. 19, no. 5, pp. 791–795, 2020.

[16] L. Sun, Y. Li, Z. Zhang, and Z. Feng, "Wideband 5G MIMO antenna with integrated orthogonal-mode dual-antenna pairs for metal-rimmed smartphones," *IEEE Trans. Antennas Propag.*, vol. 68, no. 4, pp. 2494-2503, April 2020.

[17] A. Ren, Y. Liu, and C.-Y.-D. Sim, "A compact building block with two shared-aperture antennas for eight-antenna MIMO array in metal-rimmed smartphone," *IEEE Trans. Antennas Propag.*, vol. 67, no. 10, pp. 6430–6438, Oct. 2019.

[18] K.-L. Wong, B.-W. Lin, and S.-E. Lin, "High-isolation conjoined loop multi-input multi-output antennas for the fifth-generation tablet device," *Microw. Opt. Technol. Lett.*, vol. 61, no. 1, pp. 111–119, Jan. 2019.

[19] Z. Ying, "Antennas in cellular phones for mobile communications," *Proc. IEEE*, vol. 100, no. 7, pp. 2286–2296, Jul. 2012.

[20] M. Pelosi, M. B. Knudsen, and G. F. Pedersen, "Multiple antenna systems with inherently decoupled radiators," *IEEE Trans. Antennas Propag.*, vol. 60, no. 2, pp. 503-515, Feb. 2012.

[21] Karaboikis, Soras, Tsachtsiris, and Makios, "Compact dual-printed inverted-F antenna diversity systems for portable wireless devices," *IEEE Antennas Wireless Propag. Lett.*, vol. 3, pp. 9-14, 2004.

[22] J. Deng, J. Li, L. Zhao, and L. Guo, "A dual-band inverted-F MIMO antenna with enhanced isolation for WLAN applications," *IEEE Antennas Wireless Propag. Lett.*, vol. 16, pp. 2270-2273, 2017.

[23] L. Zhao and K.-L. Wu, "A decoupling technique for four-element symmetric arrays with reactively loaded dummy elements," *IEEE Trans. Antennas Propag.*, vol. 62, no. 8, pp. 4416-4421, Aug. 2014.

[24] H. Xu, H. Zhou, S. Gao, H. Y. Wang, and Y. J. Cheng, "Multi-mode decoupling technique with independent tuning characteristic for mobile terminals," *IEEE Trans. Antennas Propag.*, vol. 65, no. 12, pp. 6739-6751, Dec. 2017.

[25] C. Deng, D. Liu, and X. Lv, "Tightly arranged four-element MIMO antennas for 5G mobile terminals," *IEEE Trans. Antennas Propag.*, vol. 67, no. 10, pp. 6353–6361, Oct. 2019.

[26] X.-T. Yuan, Z. Chen, T. Gu, and T. Yuan, "A wideband PIFA-pair-based MIMO antenna for 5G smartphones," *IEEE Antennas Wireless Propag. Lett.*, vol. 20, no.3, pp. 371-375, 2021.

[27] J. Sui and K.-L. Wu, "Self-curing decoupling technique for two inverted-F antennas with capacitive loads," *IEEE Trans. Antennas Propag.*, vol. 66, no. 3, pp. 1093-1101, Mar. 2018.

[28] J. Sui, C. Huang, and Y.-F. Cheng, "Multi-element fully-decoupled inverted-F antennas for mobile terminals," *IEEE Trans. Antennas Propag.*, vol. 70, no. 11, pp. 10076-10085, Nov. 2022.

[29] X. Zhao, S. P. Yeo, and L. C. Ong, "Decoupling of inverted-F antennas with high-order modes of ground plane for 5G mobile MIMO platform," *IEEE Trans. Antennas Propag.*, vol. 66, no. 9, pp. 4485-4495, Sept. 2018.